Detection of Klatskin's Tumor in Extrahepatic Bile Duct Strictures Using Delayed ^{18}F-FDG PET/CT: Preliminary Results for 22 Patient Studies

Michael J. Reinhardt, MD[1]; Holger Strunk, MD[2]; Thomas Gerhardt, MD[3]; Roland Roedel, MD, PhD[1]; Ursula Jaeger, MD[2]; Jan Bucerius, MD[1]; Tilman Sauerbruch, MD[3]; Hans-Juergen Biersack, MD[1]; and Franz L. Dumoulin, MD[3]

[1]Department of Nuclear Medicine, University Hospital Bonn, Bonn, Germany; [2]Department of Radiology, University Hospital Bonn, Bonn, Germany; and [3]Department of Internal Medicine I, University Hospital Bonn, Bonn, Germany

Detection of cholangiocarcinoma in extrahepatic bile duct strictures is a continuing challenge in clinical practice because brush cytology taken at endoscopic retrograde cholangiography has an average sensitivity of 50%. The aim of this study was to evaluate the effectiveness of dual-modality PET/CT using ^{18}F-FDG for noninvasive differentiation of extrahepatic bile duct strictures. **Methods:** Twenty-two PET/CT studies were performed on 20 patients (10 women, 10 men; mean age $\pm$ SD, 63 $\pm$ 14 y) with extrahepatic bile duct strictures on endoscopic retrograde cholangiography. PET imaging was started 101 $\pm$ 22 min after injection of 369 $\pm$ 48 MBq of ^{18}F-FDG. Blood glucose was 100 $\pm$ 20 mg/dL. PET images were reconstructed iteratively with attenuation correction based on a rescaling of the CT image. CT was performed within 1 min before the PET study, with the patient in the same position. CT was used to place a volume of interest 5 cm in diameter at the liver hilus for quantitative evaluation of PET images by means of standardized uptake values (SUVs). **Results:** Final diagnosis was histologically proven cholangiocarcinoma in 14 cases and benign causes of strictures in 8 cases without evidence of malignancy during a follow-up of 18 $\pm$ 3 mo. All patients with cholangiocarcinoma presented with focal increased uptake in the liver hilus with an SUV of 6.8 $\pm$ 3.3 (range, 3.9–15.8), compared with 2.9 $\pm$ 0.3 (range, 2.5–3.3) in patients with benign causes of strictures (P = 0.003). There was a clear cutoff SUV of 3.6 for detection of malignancy in the liver hilus. **Conclusion:** ^{18}F-FDG PET/CT provided high accuracy for noninvasive detection of perihilar cholangiocarcinoma in extrahepatic bile duct strictures.
Key Words: FDG; PET; CT; cholangiocarcinoma

J Nucl Med 2005; 46:1158–1163

Klatskin's tumor, or perihilar cholangiocarcinoma involving the bifurcation of the hepatic duct, accounts for approximately 70% of all bile duct cancers (*1*). More than 95% of all cancers of the biliary tree are adenocarcinomas (*2*). Cholangiocarcinoma is a well-known complication of primary sclerosing cholangitis (PSC). Nonetheless, differentiation of cholangiocarcinoma in extrahepatic bile duct strictures found on endoscopic retrograde cholangiography (ERC) or percutaneous transhepatic cholangiography is a continuing diagnostic challenge in clinical practice. The average prevalence of cholangiocarcinoma in PSC patients is about 10% (*3*). Tissue diagnosis by brush cytology taken at cholangiography is highly specific, but sensitivity has been reported to be between 18% and 70%, averaging 50% (*4–6*). Often, a combination of methods is recommended, including ERC with brush cytology, DNA analysis, and serum analysis of CA 19-9 and carcinoembryonic antigen, yielding an increased sensitivity of 70%–80% (*4,7,8*). MRI, CT, magnetic resonance cholangiopancreatography, and endoscopic ultrasonography might provide further valuable information; the exact extent of invasion, however, may be difficult to discern (*3,9*). Despite all the methodologic improvements in diagnostic imaging in the past decade, diagnosis of cholangiocarcinoma, especially in PSC, sometimes remains uncertain until invasive and aggressive approaches such as explorative laparotomy have provided a biopsy sample for histologic examination. Thus, identification of a sensitive and specific imaging modality would be a useful adjunct to existing procedures for detection of cholangiocarcinoma.

PET using ^{18}F-FDG is a noninvasive imaging method for assessment of glucose metabolism in a variety of malignancies, including adenocarcinomas, and CT is the most frequently used cross-sectional imaging technique for morphologic tumor detection (*10*). The combination of both

functional and morphologic cross-sectional imaging has been considered a new road map for imaging studies in oncology, with CT adding the anatomic details that PET lacks (*11*).

The purpose of this study was to evaluate the effectiveness of combined PET/CT for noninvasive differentiation of extrahepatic bile duct strictures.

MATERIALS AND METHODS

Patients

Between December 2002 and June 2004, 22 whole-body ^{18}F-FDG PET/CT studies were performed on 20 consecutive patients (10 women, 10 men; mean age ± SD, 63 ± 14 y) with extrahepatic bile duct strictures on ERC suggesting the presence of cholangiocarcinoma. The ERC findings included a lengthy stricture with an irregular margin and asymmetric narrowing. Extrahepatic bile duct strictures were classified according to Bismuth et al. (*12*). The median interval between ERC and ^{18}F-FDG PET/CT was 6 d (range, 3–14 d). Seven PET/CT studies were performed on patients with cytologic findings of cholangiocarcinoma for primary staging before surgical or photodynamic therapy (PDT). Eight PET/CT studies were performed on patients with PSC or other benign causes of strictures and with negative cytology findings in order to exclude cholangiocarcinoma and avoid surgery in cases of negative PET findings. Seven studies were performed on patients for therapy control after PDT of cholangiocarcinoma. PSC was diagnosed according to typical cholangiographic findings of multiple strictures and dilatations of the intra- or extrahepatic bile ducts and other published diagnostic criteria (*13*). All patients provided written consent after the nature of the imaging study had been fully explained.

Imaging Studies

All imaging studies were performed on a PET/CT scanner (Biograph; Siemens Medical Solutions, Inc.) with a 15.8-cm axial field of view and an in-plane spatial resolution of 4.6 mm. PET imaging was started 101 ± 22 min after intravenous injection of 369 ± 48 MBq of ^{18}F-FDG through an anterior cubital vein. Blood glucose measured before injection was 100 ± 20 mg/dL. The acquisition time was 5 min per bed position, with 5–7 bed positions covering thorax, abdomen, and pelvis. CT was performed within 1 min before PET with the patient in the same position. The acquisition parameters for dual-detector helical CT were 130 kV, 40 mAs, 0.8 s per CT rotation, 5-mm slice thickness, and a pitch of 1.5. One liter of an oral contrast agent was ingested within 1 h before CT for better delineation of adjacent intestinal structures. Attenuation correction for PET was based on a rescaling of the CT image as described elsewhere (*14*). No intravenous contrast agent was given, to avoid possible reconstruction artifacts on PET images of the liver (*15*). CT was used to define a perihilar volume of interest (VOI) 5 cm in diameter for quantitative evaluation of PET images. Maximum standardized uptake value (SUV$_{max}$ = activity concentration/injected dose/body weight) was obtained for the perihilar VOI of each patient. Because SUV$_{max}$ might represent the peak activity of only a single voxel, a 75% isocontour area within the perihilar VOI was defined to determine the 75% SUV (SUV$_{75\%}$). Mean SUV$_{max}$ and SUV$_{75\%}$ were compared between patients with and without Klatskin's tumor. Quantitative evaluation of PET images was performed using e.soft 3.0 software (Siemens Medical Solutions, Inc.).

Statistical Analysis

Mean values and SDs, as well as 95% confidence interval of the mean of SUV$_{max}$ and SUV$_{75\%}$, are given for patients with perihilar cholangiocarcinoma and with benign causes of strictures. The comparison of mean SUV$_{max}$ and SUV$_{75\%}$ between patients with and without Klatskin's tumor was performed by means of 1-way ANOVA and displayed as box plots. All statistical evaluation was done using SPSS 12.0 software (SPSS Inc.) for Windows (Microsoft).

RESULTS

^{18}F-FDG PET Findings and Clinical Course of Disease

Perihilar adenocarcinoma of the bile ducts was confirmed histologically in all patients who underwent ^{18}F-FDG PET/CT before surgical or PDT treatment. All these patients had focal increased ^{18}F-FDG uptake in the liver hilus. The tumors included 3 Bismuth IV and 2 each Bismuth II and III tumors, with 5 being American Joint Committee on Cancer (AJCC) stage II and 2 being AJCC stage III.

Seven of 8 patients with suspected benign causes of strictures had no evidence of malignancy during further follow-up of 18 ± 3 mo (range, 12–21 mo) and had no perihilar increased metabolic activity. In the eighth patient, cholangiocarcinoma was suspected at ERC but several biopsy specimens taken at that time were negative. This patient (patient 12) had perihilar increased ^{18}F-FDG uptake with an SUV$_{max}$ of 4.2 and an SUV$_{75\%}$ of 3.5 on ^{18}F-FDG PET/CT. Therefore, she underwent partial resection of the liver 1–2 wk later, and cholangiocarcinoma was then confirmed histologically.

Seven PET/CT studies were performed on 6 patients for therapy control after PDT of Klatskin's tumor; all tumors were Bismuth IV. Four patients had persisting perihilar hypodensity, and 2 patients showed tumor regression on CT. However, 5 of them had focal increased ^{18}F-FDG uptake, including 1 of the 2 patients with decreasing tumor size on CT. All patients with focal increased ^{18}F-FDG uptake experienced disease relapse within 5–14 mo, whereas the 1 patient lacking ^{18}F-FDG uptake in the liver hilus had no evidence of remaining or recurrent malignancy at the end of 18 mo of follow-up. The ^{18}F-FDG PET/CT study of this patient (patient 20) is shown in Figure 1. Figure 2 shows the ^{18}F-FDG PET/CT study of patient 11, who had a partial response after PDT on CT but had increased ^{18}F-FDG uptake in the remaining tumor and experienced relapse of disease 14 mo later.

Further details on patients, including indications for ^{18}F-FDG PET/CT studies, results of quantitative analysis, histology, and outcome, are shown in Table 1.

Quantitative Evaluation of ^{18}F-FDG PET/CT

The perihilar SUV$_{max}$ of patients without cholangiocarcinoma was 2.87 ± 0.25, with minimum and maximum values of 2.47 and 3.24 and a 95% confidence interval of 2.66–3.08. The perihilar SUV$_{max}$ of patients with Klatskin's tumor was 6.81 ± 3.3, with minimum and maximum values of 3.85 and 15.8 and a 95% confidence interval of 4.89–
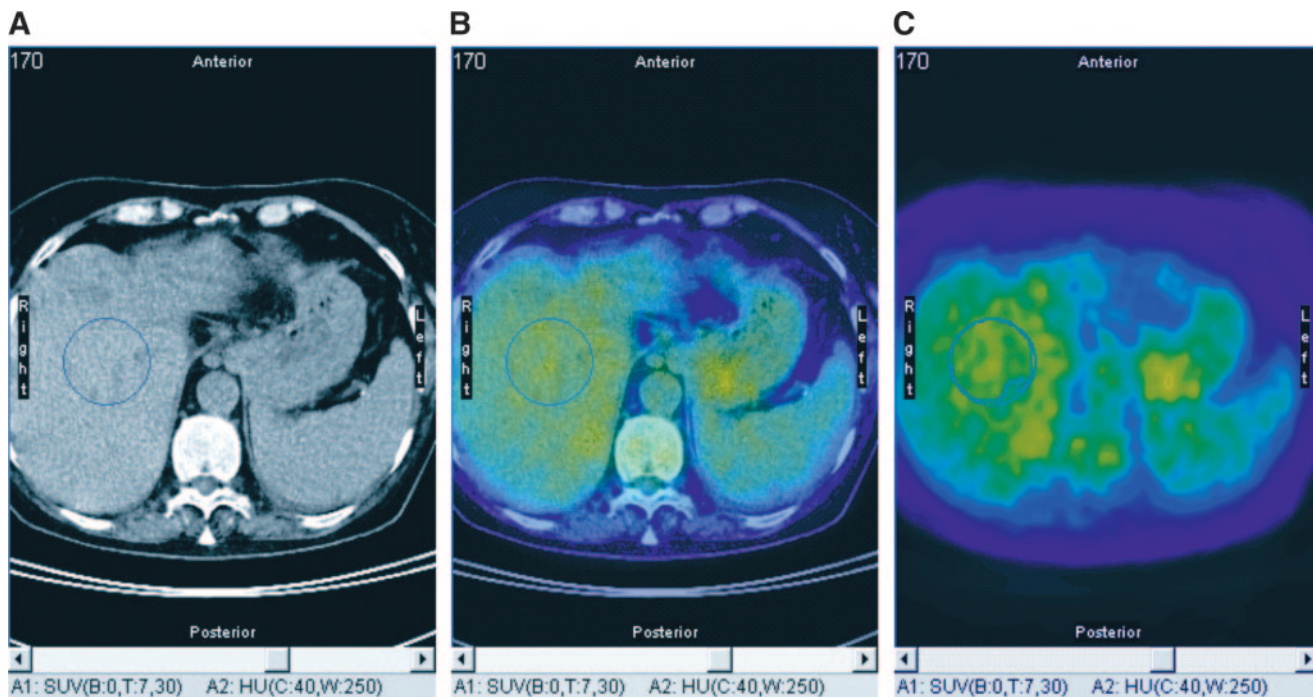
FIGURE 1. ^{18}F-FDG PET/CT of patient with no evidence of malignancy after PDT. (A) Native CT image shows discrete hypodense areas in liver segments 4B and 5. (B) Fused image (CT, 50%; PET, 50%) enables anatomic correlation of glucose metabolism. (C) ^{18}F-FDG PET image shows 75% and 100% isocontour areas used for SUV analysis (SUV$_{max}$ = 3.2 and SUV$_{75\%}$ = 2.5). Note atrophy of left liver lobe.

8.72. The geometric and arithmetic means between the highest SUV$_{max}$ of patients without cholangiocarcinoma and the lowest SUV$_{max}$ of patients with cholangiocarcinoma were 3.54 and 3.55, respectively. Thus, an SUV$_{max}$ of 3.6 was defined as the cutoff for detection of malignancy in central bile duct strictures. Using the isocontour SUV$_{75\%}$ in the anatomically defined perihilar VOI, the SUV$_{75\%}$ of patients without cholangiocarcinoma was 2.32 ± 0.19, with
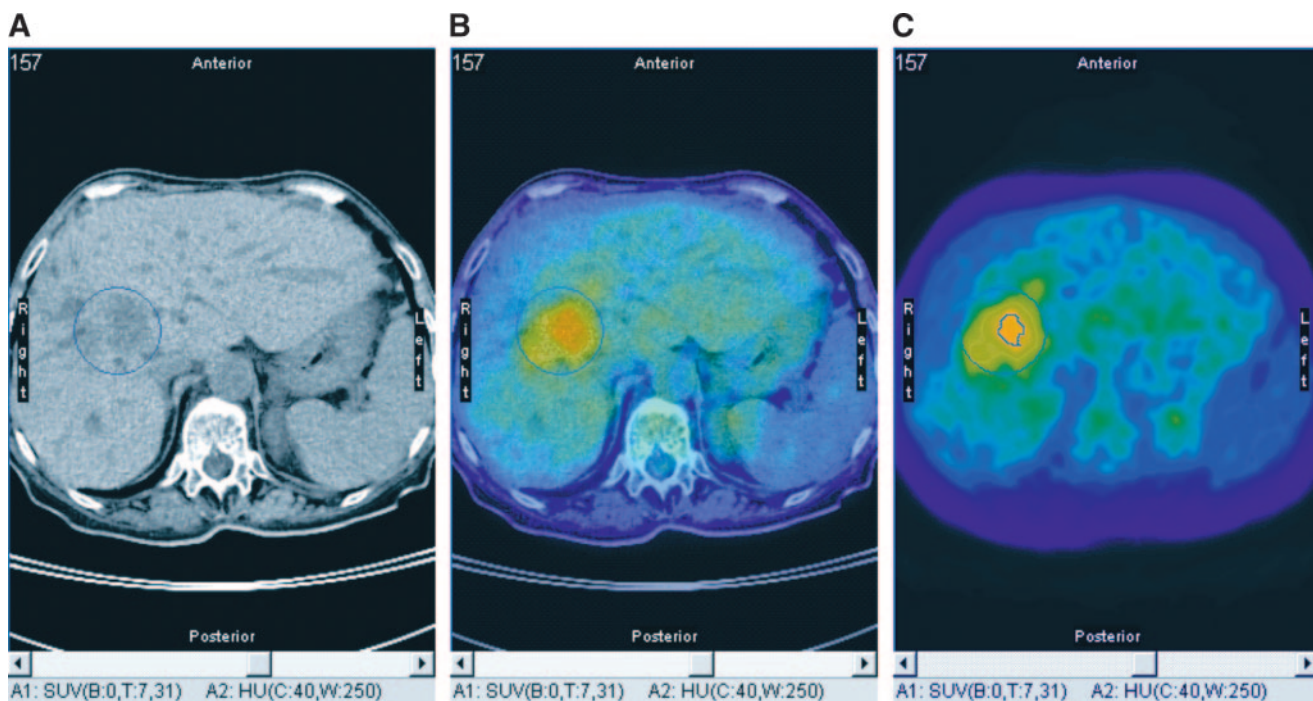

FIGURE 2. ^{18}F-FDG PET/CT of patient with residual Klatskin's tumor after PDT and Yamakawa stent implantation. (A) Native CT image shows large hypodense area in liver hilus. (B) Fused image (CT, 50%; PET, 50%) enables anatomic correlation of increased glucose metabolism. (C) ^{18}F-FDG PET image shows 75% and 100% isocontour areas used for SUV analysis (SUV$_{max}$, 5.0, and SUV$_{75\%}$, 4.1).

TABLE 1
Characteristics, ^{18}F-FDG PET/CT Indications, Perihilar SUV, Histology, and Outcome
of 20 Patients with Extrahepatic Bile Duct Strictures

Patient no.	Age (y)	Sex	Indication for ^{18}F-FDG PET/CT	Perihilar SUV_{max}	Perihilar $SUV_{75\%}$	Histology	Outcome
1	63	F	Staging before surgery	3.9	3.1	CC	Curative resection
2	46	M	Staging before surgery	5.2	4.3	CC	Curative resection
3	68	M	Staging before surgery	6.1	5.1	CC	Curative resection
4	66	F	Staging before surgery	6.6	5.6	CC	Curative resection
5	71	M	Staging before PDT	5.2	4.2	CC	Stable disease
6	75	M	Staging before PDT	6.3	5.2	CC	Stable disease
7	76	M	Staging before PDT	9.8	8.2	CC	Stable disease
			Tx control after PDT	11.0	9.0	CC	Disease progress on CT 5 mo later
8	77	F	Tx control after PDT	15.8	11.8	CC	Disease progress on CT 6 mo later
9	76	M	Tx control after PDT	5.2	4.3	CC	Stable disease for 6 mo
			Follow-up after 6 mo	7.1	5.9	CC	Disease progress on CT 7 mo later
10	61	F	Tx control after PDT	3.9	3.2	CC	Disease progress on CT 9 mo later
11	64	F	Tx control after PDT	5.0	4.1	CC	Disease progress on CT 14 mo later
12	78	F	Exclusion of CC*	4.2	3.5	CC	Curative resection
13	64	M	Exclusion of CC*	3.2	2.7	No CC	12-mo follow-up negative
14	82	F	Exclusion of CC*	2.7	2.2	No CC	18-mo follow-up negative
15	59	M	Exclusion of CC*	3.0	2.2	No CC	20-mo follow-up negative
16	63	M	Exclusion of CC*	2.9	2.3	No CC	21-mo follow-up negative
17	60	M	PSC, exclusion of CC*	3.1	2.4	No CC	18-mo follow-up negative
18	35	F	PSC, exclusion of CC*	2.7	2.2	No CC	19-mo follow-up negative
19	37	F	PSC, exclusion of CC*	2.5	2.1	No CC	20-mo follow-up negative
20	71	F	Tx control after PDT of CC	3.0	2.5	No CC	18-mo follow-up negative

————

*To avoid surgery when ^{18}F-FDG PET/CT gave no evidence of malignancy.

CC = cholangiocarcinoma; Tx = therapy.

minimum and maximum values of 2.08 and 2.66 and a 95% confidence interval of 2.17–2.48. The perihilar $SUV_{75\%}$ of patients with Klatskin's tumor was 5.61 ± 2.69, with minimum and maximum values of 3.13 and 12.8 and a 95% confidence interval of 4.06–7.17. The geometric and arithmetic means between the highest $SUV_{75\%}$ of patients without cholangiocarcinoma and the lowest $SUV_{75\%}$ of patients with cholangiocarcinoma were 2.885 and 2.895, respectively. Thus, an $SUV_{75\%}$ of 2.9 was defined as the cutoff for detection of malignancy in central bile duct strictures.

The differences in SUV_{max} and $SUV_{75\%}$ between patients with and without cholangiocarcinoma were significant: $P = 0.003$ for SUV_{max} and $P = 0.003$ for $SUV_{75\%}$. The distribution of SUV_{max} in patients with and without Klatskin's tumor is shown in Figure 3, and that of $SUV_{75\%}$ is shown in Figure 4.

DISCUSSION

The usefulness of ^{18}F-FDG PET for detection of cholangiocarcinoma has been shown in just a few studies, most of them including fewer than 20 patients (16–20). The first 2 studies did not specifically address cholangiocarcinoma but rather assessed malignant lesions of different origins in the liver, including hepatocellular carcinoma and liver metastases from colon carcinoma, in comparison with normal liver tissue (16,17). In 1992, Okazumi et al. performed dynamic
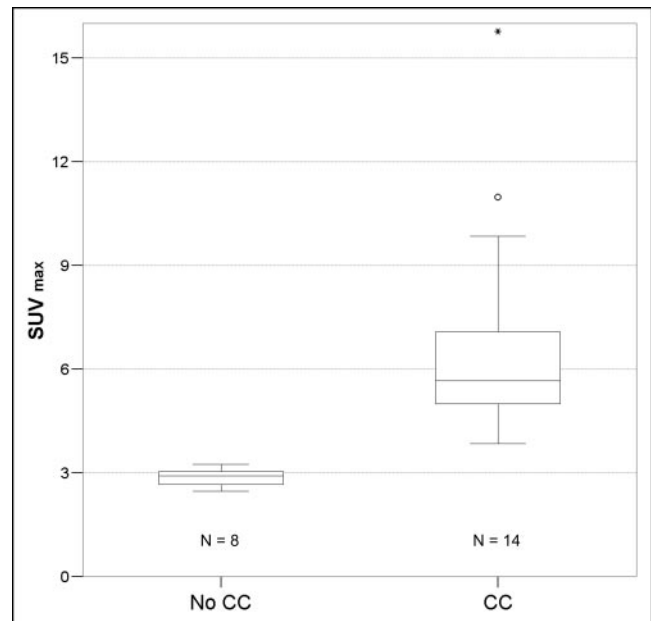
FIGURE 3. Box plot analysis of perihilar SUV_{max} in 22 patient studies with and without cholangiocarcinoma. ○ = outliers; * = extreme cases; CC = cholangiocarcinoma.
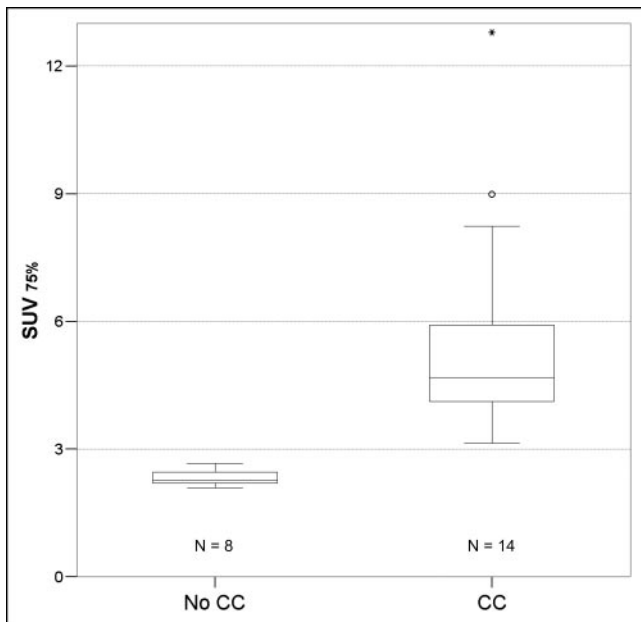
FIGURE 4. Box plot analysis of perihilar $SUV_{75\%}$ in 22 patient studies with and without cholangiocarcinoma. $\bigcirc$ = outliers; * = extreme cases; CC = cholangiocarcinoma.

^{18}F-FDG PET studies that included arterial blood sampling until 60 min after intravenous injection of the radiotracer (*16*). They observed a higher ^{18}F-FDG uptake in the tumors than in the surrounding liver tissue at 60 min after injection and defined a k3-value (which describes the phosphorylative activity of hexokinase) of ≥0.025 as indicative of malignancy.

In 1998, Delbeke et al. studied 8 patients with cholangiocarcinoma (*17*). All had increased target-to-nontarget ratios (>2). SUV_{max} was 7.2 ± 3.2, with PET begun 68 ± 33 min after injection. The investigators concluded that conventional static ^{18}F-FDG PET can distinguish malignant lesions in the liver. Also in 1998, Keiding et al. compared, for the first time, ^{18}F-FDG liver uptake in patients with PSC but no cholangiocarcinoma, patients with PSC and cholangiocarcinoma, and patients with no liver disease (*18*). The investigators performed dynamic PET scanning of the liver for 90 min after injection of the radiotracer and included arterial blood sampling. Quantitative analysis was done by means of a VOI covering all voxels that enclosed at least 75% of the maximum radioactivity concentration. Using an estimate of the net metabolic clearance of ^{18}F-FDG, K (in mL of plasma min^{-1} mL^{-1} of tissue), Keiding et al. could clearly differentiate all PSC patients with cholangiocarcinoma from those with PSC but without cholangiocarcinoma. However, the K-values of patients with PSC were significantly higher than those of patients without liver disease, suggesting increased glucose metabolism in PSC tissue. The investigators concluded that for detecting small and early malignant tumors in the liver, morphologic imaging procedures might be less suitable than ^{18}F-FDG PET, because it revealed hot spots in areas that were not sus-

pected on ultrasound and MRI in up to half the cholangiocarcinoma patients.

In 2001, Fritscher-Ravens et al. performed ^{18}F-FDG PET, CT, and endoscopic retrograde cholangiopancreatography on 15 patients with PSC before surgical intervention (*19*). In 10 patients with adenocarcinoma of the bile ducts and tumor sizes between 0.9 and 4.5 cm, the tumors were clearly seen on ^{18}F-FDG PET images 60 min after injection of the radiotracer, in contrast to 3 patients with mucinous adenocarcinoma. Two patients with benign Klatskin-mimicking chronic inflammatory lesions had false-positive PET findings, with target-to-nontarget ratios similar to those of cholangiocarcinoma. The authors suggested that ^{18}F-FDG PET is more useful for the detection of distant metastases than for differentiation of malignant from benign lesions in the liver. In the same year, Kluge et al. performed ^{18}F-FDG PET on 26 patients with adenocarcinomas of the bile ducts, 8 patients with benign lesions of the biliary tree, and 20 patients with no liver disease (*20*). Kluge et al. visually and quantitatively analyzed mean SUV in a 90% isocontour area around the most intense focus of uptake in the liver, with PET begun 50 min after injection of the radiotracer. In that study, visual analysis discriminated malignant from benign lesions significantly better than did SUV analysis, with an area under the receiver operating characteristic curve of 0.96 for visual analysis, compared with 0.87 for SUV analysis ($P < 0.05$). This difference disappeared after normalization of tumor SUV to that of normal liver tissue, which might be explained by higher ^{18}F-FDG uptake in livers of PSC patients than in those of healthy controls, similarly observed in the study by Keiding et al. (*18*). A clear cutoff between malignant and benign lesions in the liver was shown in most of the quantitatively evaluated PET studies, that is, in the dynamic PET studies of Okazumi et al. (*16*) and Keiding et al. (*18*), in the SUV-based analysis of Delbeke et al. (*17*), and in our data.

The SUV_{max} cutoff for detection of cholangiocarcinoma was essentially the same in our study and the study of Delbeke et al. (*17*). In the Delbeke study it was >3.5, and in our study it was 3.6. The different uptake periods (101 ± 22 min vs. 68 ± 33 min) and acquisition times (5 min vs. 15 min per bed position) in our study and the Delbeke study would have led to the liver's coming into the field of view at a similar time in both studies, about 110–120 min after injection. This would explain the similar cutoff of SUV for detection of cholangiocarcinoma in the liver in both studies, as the tumor uptake of ^{18}F-FDG might change with time (*21*). However, the significantly reduced scanning time of ^{18}F-FDG PET/CT increased patient comfort and enabled late acquisition without significantly interfering with departmental operations.

Several human and experimental studies found that a late imaging time for ^{18}F-FDG PET better discriminated between tumor and inflammation (*22–25*). However, one cannot rule out the possibility that a few cases of focal granulomatous inflammation in the liver might give false-positive

^{18}F-FDG PET findings, especially when PET is performed within 60–90 min after injection (*19,20*). In addition, false-negative ^{18}F-FDG PET/CT results might be obtained when one is studying the rare subtype of mucinous carcinomas of the biliary tree, which seems not to show increased ^{18}F-FDG uptake (*19*).

Despite our not using the full potential of the CT scan, since we did not administer intravenous contrast agents, we observed an improved anatomic localization of positive ^{18}F-FDG PET findings rarely achievable with the standard 511-keV transmission images of a PET scanner (*15*). The direct incorporation of anatomic information derived from CT data into PET image reconstruction may be advantageous, since attenuation correction is essential for quantitative evaluation of PET images (*26*). Specifically, CT offers improved contrast and resolution and much lower statistical noise than do the standard 511-keV transmission images, especially for whole-body PET (*15*). In the present study, the anatomic information from the CT scan was used to define a VOI for quantitative evaluation of the liver hilus. By means of this advanced technique, ^{18}F-FDG PET/CT differentiated 12 patients with cholangiocarcinoma from 8 patients without cholangiocarcinoma. These included 1 patient with repeatedly negative biopsy results, in whom ^{18}F-FDG PET/CT was the first diagnostic procedure to give evidence of malignancy, which was then confirmed histologically a few weeks later when the patient underwent surgery. Furthermore, disease progression after PDT was correctly predicted with ^{18}F-FDG PET/CT in all patients, including one for whom morphologic imaging procedures demonstrated tumor regression. In that patient, the combination of decrease in tumor size on CT and positive ^{18}F-FDG PET findings suggested late relapse. And finally, ^{18}F-FDG PET/CT correctly identified all patients with PSC and other benign causes of strictures in whom cholangiocarcinoma did not develop within the following 18 mo, including 1 patient without evidence of recurrent malignancy after PDT of cholangiocarcinoma.

CONCLUSION

^{18}F-FDG PET/CT of the liver performed late—about 120 min after injection—might play a significant role in noninvasive detection and therapy control of Klatskin's tumor.

ACKNOWLEDGMENT

REFERENCES

1. Klatskin G. Adenocarcinoma of the hepatic duct at its bifurcation within the porta hepatis: an unusual tumor with distinctive clinical and pathological features. *Am J Med.* 1965;38:241–256.
2. Pitt HA, Grochow LB, Abrams RA. Cancer of the biliary tree. In: DeVita VT, Hellman S, Rosenberg SA, eds. *Cancer: Principles and Practice of Oncology.* 5th ed. Philadelphia, PA: Lippincott-Raven Publishers; 1997:1114–1128.
3. De Groen PC, Gores GJ, LaRusso NF, Gunderson LL, Nagorney DM. Biliary tract cancers. *N Engl J Med.* 1999;341:1368–1378.
4. Siqueira E, Schoen RE, Silverman W, et al. Detecting cholangiocarcinoma in patients with primary sclerosing cholangitis. *Gastrointest Endosc.* 2002;56:40–47.
5. Jailwala J, Fogel EL, Sherman S, et al. Triple-tissue sampling at ERCP in malignant biliary obstruction. *Gastrointest Endosc.* 2000;51:383–390.
6. Glasbrenner B, Ardan M, Boeck W, Preclik G, Moller P, Adler G. Prospective evaluation of brush cytology of biliary strictures during endoscopic retrograde cholangiopancreatography. *Endoscopy.* 1999;31:712–717.
7. Lindberg B, Arnelo U, Bergquist A, et al. Diagnosis of biliary strictures in conjunction with endoscopic retrograde cholangiopancreaticography, with special reference to patients with primary sclerosing cholangitis. *Endoscopy.* 2002;34:909–916.
8. van Leeuwen DJ, Reeders JW. Primary sclerosing cholangitis and cholangiocarcinoma as a diagnostic and therapeutic dilemma. *Ann Oncol.* 1999;10(suppl 4):89–93.
9. Park MS, Kim TK, Kim KW, et al. Differentiation of extrahepatic bile duct cholangio-carcinoma from benign stricture: findings at MRCP versus ERCP. *Radiology.* 2004;233:234–240.
10. Gambhir SS, Czernin J, Schwimmer J, Silverman DHS, Coleman RE, Phelps ME. A tabulated summary of the FDG PET literature. *J Nucl Med.* 2001;42(suppl):1–93.
11. Ell PJ, von Schulthess GK. PET/CT: a new road map. *Eur J Nucl Med Mol Imaging.* 2002;29:719–720.
12. Bismuth H, Nakache R, Diamond T. Management strategies in resection for hilar cholangiocarcinoma. *Ann Surg.* 1992;215:31–38.
13. Lee YM, Kaplan MM. Primary sclerosing cholangitis. *N Engl J Med.* 1995;332:924–933.
14. Beyer T, Townsend DW, Brun T, et al. A combined PET/CT scanner for clinical oncology. *J Nucl Med.* 2000;41:1369–1379.
15. Kinahan PE, Hasegawa BH, Beyer T. X-ray-based attenuation correction for positron emission tomography/computed tomography scanners. *Semin Nucl Med.* 2003;33:166–179.
16. Okazumi S, Isono K, Enomoto K, et al. Evaluation of liver tumors using fluorine-18-fluorodeoxyglucose PET: characterization of tumor and assessment of effect of treatment. *J Nucl Med.* 1992;33:333–339.
17. Delbeke D, Martin WH, Sandler MP, Chapman WC, Wright JK Jr, Pinson CW. Evaluation of benign vs malignant hepatic lesions with positron emission tomography. *Arch Surg.* 1998;133:510–515.
18. Keiding S, Hansen SB, Rasmussen HH, et al. Detection of cholangiocarcinoma in primary sclerosing cholangitis by positron emission tomography. *Hepatology.* 1998;28:700–706.
19. Fritscher-Ravens A, Bohuslavizki KH, Broering DC, et al. FDG PET in the diagnosis of hilar cholangiocarcinoma. *Nucl Med Commun.* 2001;22:1277–1285.
20. Kluge R, Schmidt F, Caca K, et al. Positron emission tomography with [18F]fluoro-2-deoxy-D-glucose for diagnosis and staging of bile duct cancer. *Hepatology.* 2001;33:1029–1035.
21. Pauwels EK, Sturm EJ, Bombardieri E, Cleton FJ, Stokkel MP. Positron-emission tomography with [18F]fluorodeoxyglucose. Part I. Biochemical uptake mechanism and its implication for clinical studies. *J Cancer Res Clin.* 2000;126:549–559.
22. Boerner AR, Weckesser M, Herzog H, et al. Optimal scan time for fluorine-18 fluorodeoxyglucose positron emission tomography in breast cancer. *Eur J Nucl Med.* 1999;26:226–230.
23. Hustinx R, Smith RJ, Benard F, et al. Dual time point fluorine-18 fluorodeoxyglucose positron emission tomography: a potential method to differentiate malignancy from inflammation and normal tissue in the head and neck. *Eur J Nucl Med.* 1999;26:1345–1348.
24. Zhuang H, Pourdehnad M, Lambright ES, et al. Dual time point ^{18}F-FDG PET imaging for differentiating malignant from inflammatory processes. *J Nucl Med.* 2001;42:1412–1417.
25. Matthies A, Hickeson M, Cuchiara A, Alavi A. Dual time point ^{18}F-FDG PET for the evaluation of pulmonary nodules. *J Nucl Med.* 2002;43:871–875.
26. Comtat C, Kinahan PE, Fessler JA, et al. Clinically feasible reconstruction of 3D whole-body PET/CT data using blurred anatomical labels. *Phys Med Biol.* 2002;47:1–20.